Supplementary Information (SI) for New Journal of Chemistry.

Supporting Information

Noble metal free high entropy alloys with amorphous based heterostructure for oxygen evolution reaction

Jia Yao[a], Yin'an Zhu[b], Ting Dai[a], Tao Lu*[a], and Ye Pan*[a]

[a] *School of Materials Science and Engineering, Jiangsu Key Laboratory of Advanced Metallic Materials, Southeast University, Nanjing 211189, China.*

[b] *Key Laboratory of Advanced Fuel Cells and Electrolyzers Technology of Zhejiang Province, Ningbo Institute of Materials Technology and Engineering, Chinese Academy of Sciences, Ningbo, Zhejiang 315201, P.R. China*

* Correspondent Author: Ye Pan, e-mail: panye@seu.edu.cn

* Correspondent Author: Tao Lu, e-mail: lutao@seu.edu.cn

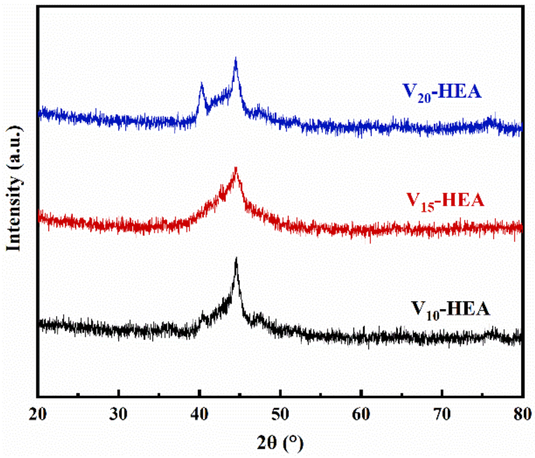

Fig S1. XRD patterns of p-V_{10}-HEA, p-V_{15}-HEA and p-V_{20}-HEA.

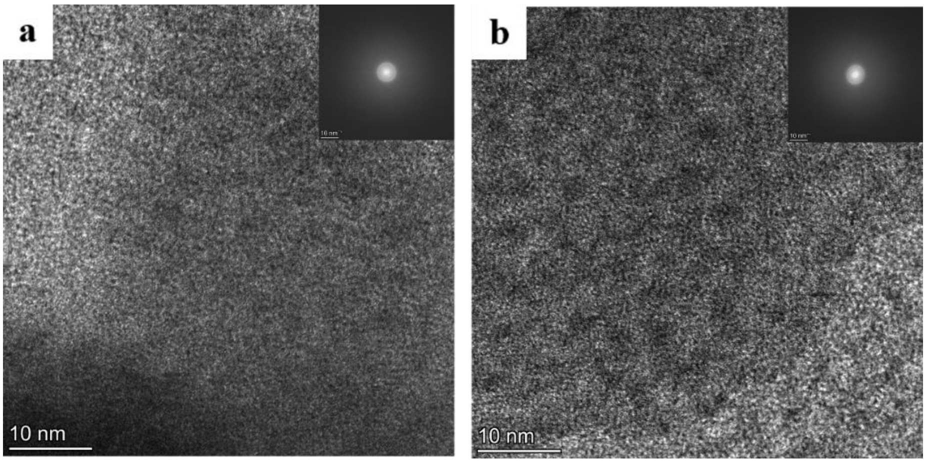

Fig S2. HRTEM images of surface layer of (a) p-V_{10}-HEA and (b) p-V_{15}-HEA. Inset images are the corresponding SEAD pattern.

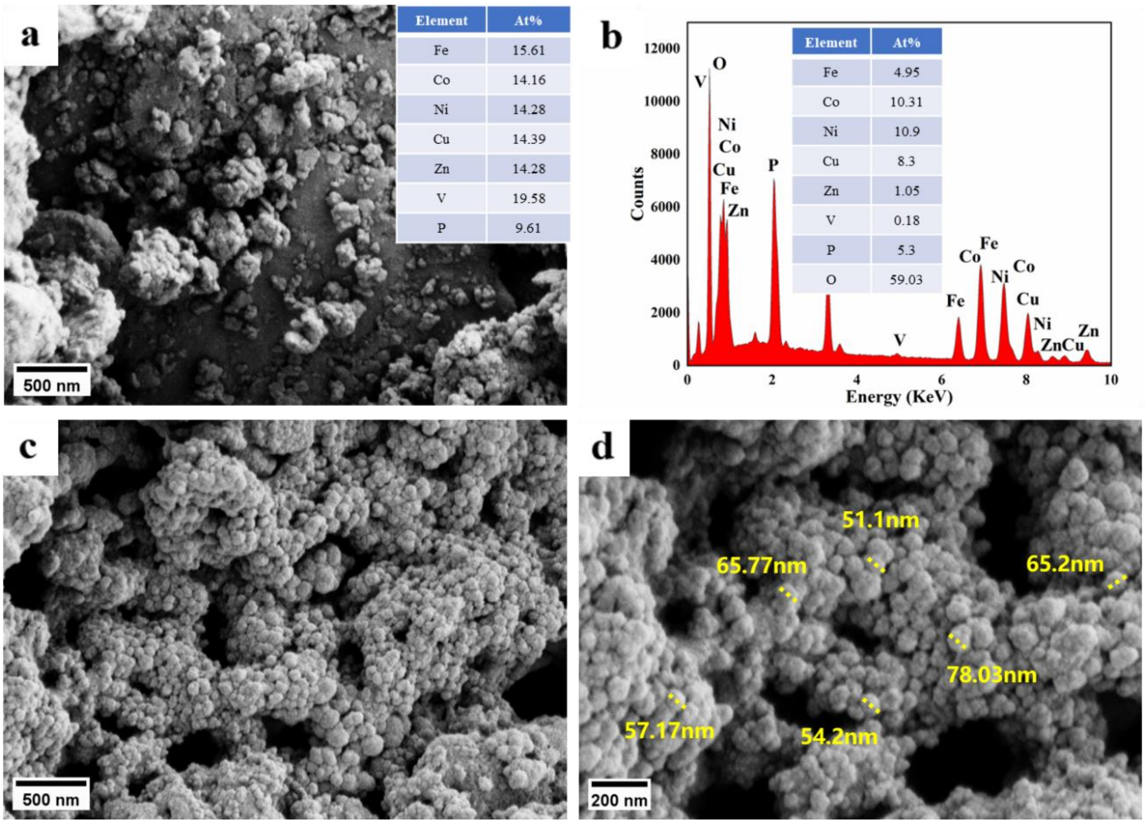

Fig S3. SEM images of (a) p-V_{20}-HEA, (b) EDX analysis of the nanoparticles formed on cv-V_{20}-HEA and (c-d) cv-V_{20}-HEA.

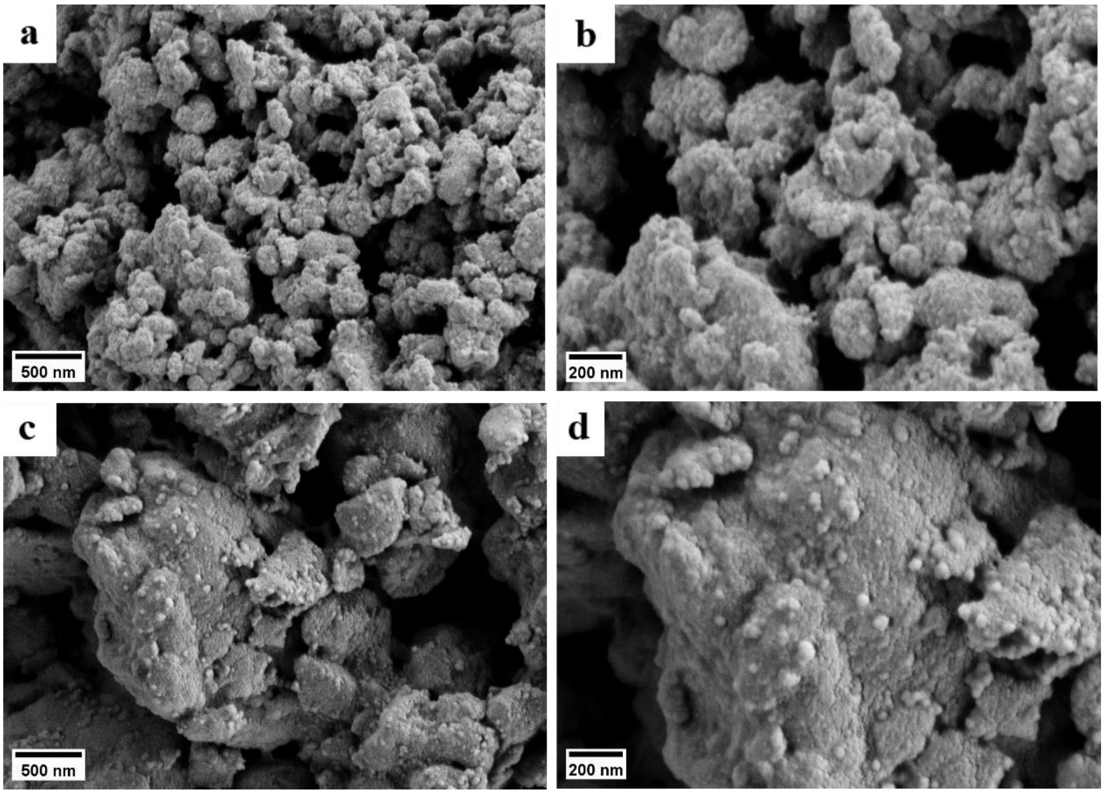

Fig S4. SEM images of (a-b) cv-V_{10}-HEA and (c-d) cv-V_{15}-HEA.

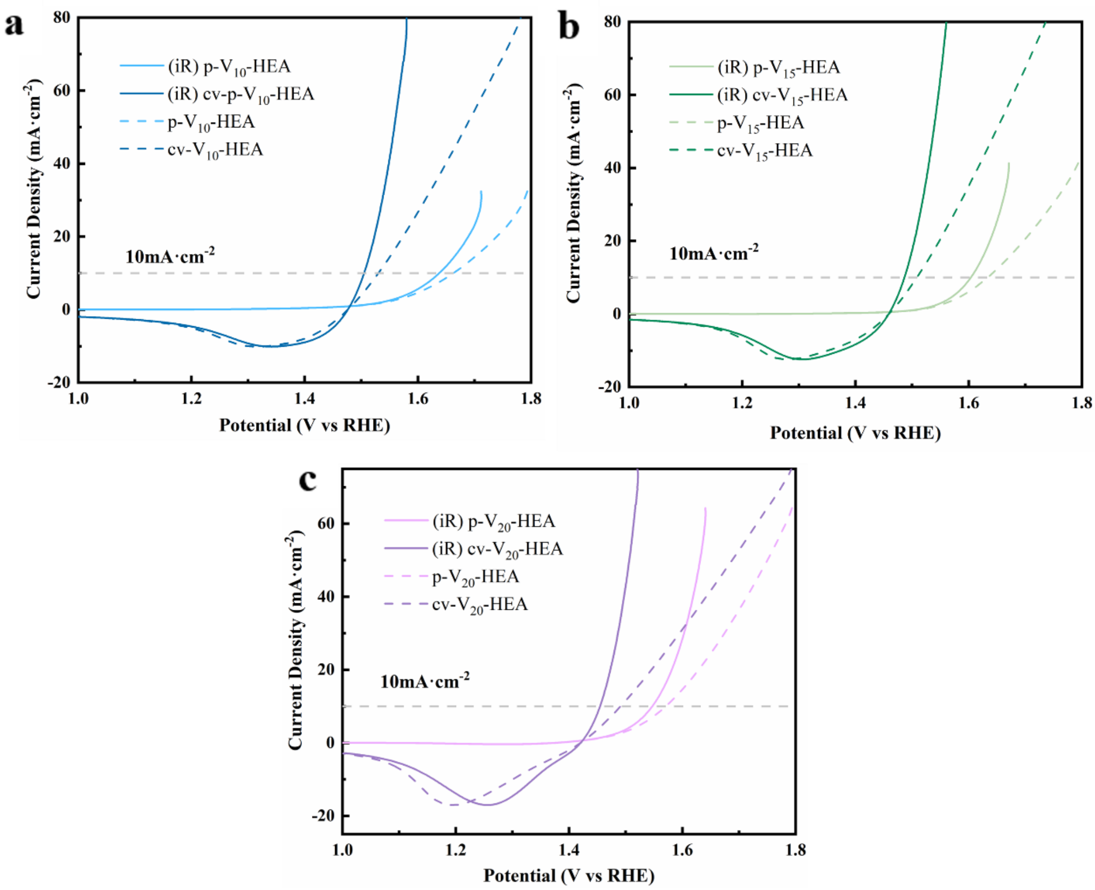

Fig S5. iR corrected LSV curves of (a) V_{10}-HEA, (b) V_{15}-HEA and (c) V_{20}-HEA.

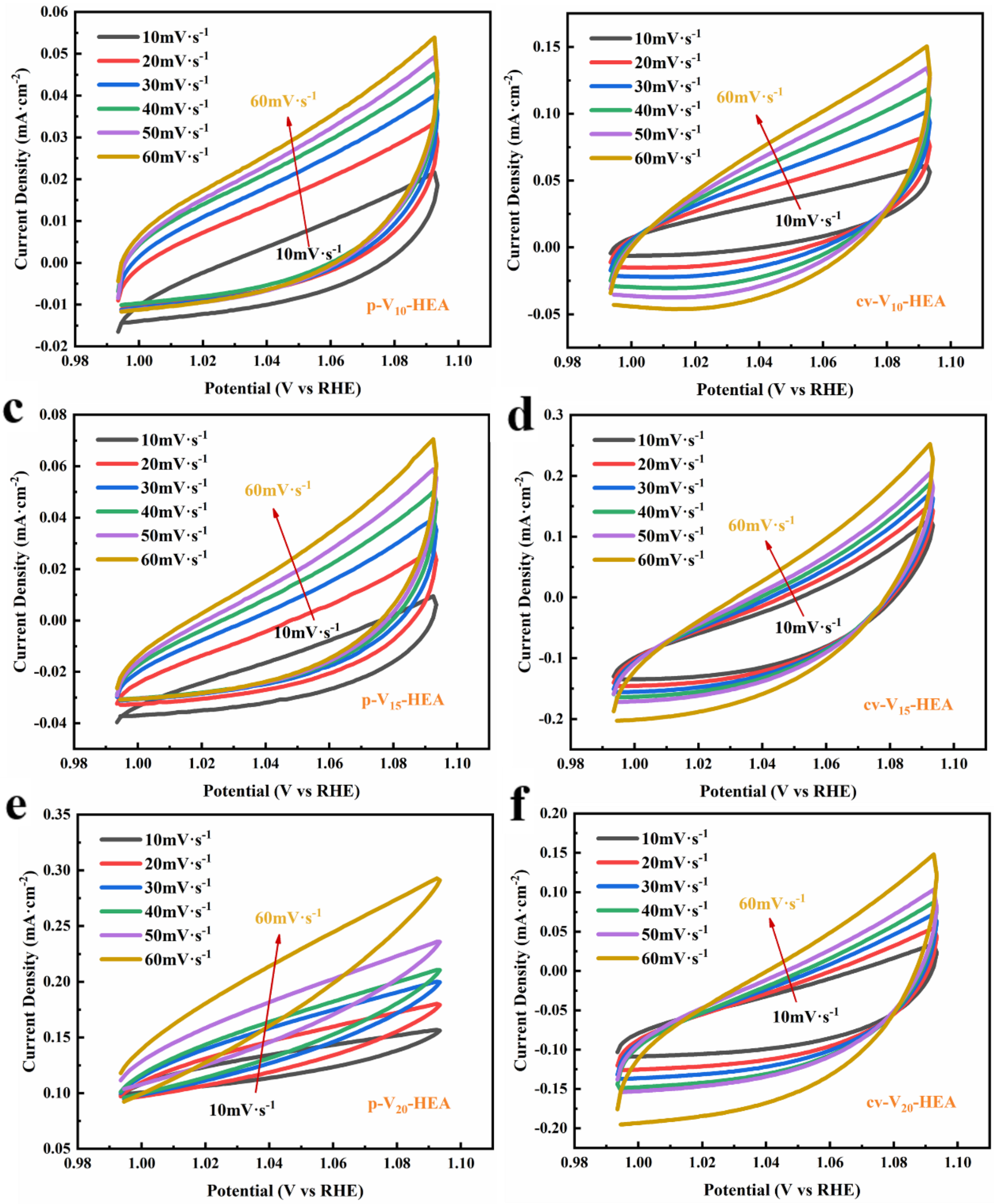

Fig S6. CV curves of (a) p-V_{10}-HEA, (b) cv-V_{10}-HEA, (c) p-V_{15}-HEA, (d) cv-V_{15}-HEA, (e) p-V_{20}-HEA and (f) cv-V_{20}-HEA at scan rates ranging from 10 mV·s^{-1} to 60·mV s^{-1} with an interval point of 20·mV s^{-1}.

Table S1. Summary of OER catalysts in recent work of literatures.

Number	Catalysts	Structural feature	Overpotential/(mV)	Tafel slope/ ($mV\cdot dec^{-1}$)	Reference
1	FeNiCuCoZnVP	Nanoparticles	$228@10mA\cdot cm^{-2}$	24	This work
2	CrMnFeCoNi)S	Nanoparticles	$295@100mA\cdot cm^{-2}$	68	[1]
3	FeCoNiCuPd	Nanoparticles	$390@10mA\cdot cm^{-2}$	96	[2]
4	NiCoFeMoMn	Nanoporous	$243@10mA\cdot cm^{-2}$	37	[3]
5	FeCoNiMnRu	Nanoparticles	$308@10mA\cdot cm^{-2}$	61.3	[4]
6	FeCoNiIrRu/ CNFs	Nanoparticles	$241@10mA\cdot cm^{-2}$	153	[5]
7	CoNiCuMnAl/C	Nanoparticles	$215@10mA\cdot cm^{-2}$	35.6	[6]
8	FeCoNiCuPd	Thin-film	$194@10mA\cdot cm^{-2}$	39.8	[7]
9	FeCoNiRu-450	Rice shape	$243@10mA\cdot cm^{-2}$	45	[8]
10	CrMnFeCoNi	Film	$287@10mA\cdot cm^{-2}$	39	[9]
11	$Al_{0.6}CrFe_2Ni_2$	Nanocrystallization	$259.5@10mA\cdot cm^{-2}$	47.9	[10]
12	CrMnFeCoNi	Nanoparticles	$265@10mA\cdot cm^{-2}$	37.9	[11]
13	ZnNiCoIrMn	Nanoporous	$237@10mA\cdot cm^{-2}$	46	[12]
14	1 P-HEA	Monolithic porous	$211@10mA\cdot cm^{-2}$	41.3	[13]
15	CoNiCuMnMo	Nanoparticles	$320@10mA\cdot cm^{-2}$	107.2	[14]
16	MnFeCoNiCu	Nanoparticles	$263@10mA\cdot cm^{-2}$	43	[15]
17	RuO_2	Nanoparticles	$342@10mA\cdot cm^{-2}$	117	This work

Reference

[1] Cui M, Yang C, Li B, et al. High-Entropy Metal Sulfide Nanoparticles Promise High-Performance Oxygen Evolution Reaction. Advanced Energy Materials, 2021, 11(3) : 2002887.

[2] Li H, Zhu H, Shen Q, et al. A novel synergistic confinement strategy for controlled synthesis of high-entropy alloy electrocatalysts. Chemical Communications, 2021, 57(21) : 2637–2640.

[3] Liu H, Qin H, Kang J, et al. A freestanding nanoporous NiCoFeMoMn high-entropy alloy as an efficient electrocatalyst for rapid water splitting. Chemical Engineering Journal, 2022, 435 : 134898.

[4] Hao J, Zhuang Z, Cao K, et al. Unraveling the electronegativity-dominated intermediate adsorption on high-entropy alloy electrocatalysts. Nature Communications, 2022, 13(1) : 2662.

[5] Zhu H, Zhu Z, Hao J, et al. High-entropy alloy stabilized active Ir for highly efficient acidic oxygen evolution. Chemical Engineering Journal, 2022, 431 : 133251.

[6] Wang S, Huo W, Fang F, et al. High entropy alloy/C nanoparticles derived from polymetallic MOF as promising electrocatalysts for alkaline oxygen evolution reaction. Chemical Engineering Journal, 2022, 429 : 132410.

[7] Wang S, Xu B, Huo W, et al. Efficient FeCoNiCuPd thin-film electrocatalyst for alkaline oxygen and hydrogen evolution reactions. Applied Catalysis B: Environmental, 2022, 313 : 121472.

[8] Huang K, Xia J, Lu Y, et al. Self-Reconstructed Spinel Surface Structure Enabling the Long-Term Stable Hydrogen Evolution Reaction/Oxygen Evolution Reaction Efficiency of FeCoNiRu

High-Entropy Alloyed Electrocatalyst. Advanced Science, 2023, 10(14) : 2300094.
[9] Chen J, Ling Y, Yu X, et al. Water oxidation on CrMnFeCoNi high entropy alloy: Improvement through rejuvenation and spin polarization. Journal of Alloys and Compounds, 2022, 929 : 167344.
[10] Zhang T, Li G, Liang J, et al. Strain-engineering-regulated Al0.6CrFe2Ni2 high entropy alloy enhances electrocatalytic water oxidation. Journal of Alloys and Compounds, 2023, 945 : 169319.
[11] He R, Yang L, Zhang Y, et al. A CrMnFeCoNi high entropy alloy boosting oxygen evolution/reduction reactions and zinc-air battery performance. Energy Storage Materials, 2023, 58 : 287–298.
[12] Kwon J, Sun S, Choi S, et al. Tailored Electronic Structure of Ir in High Entropy Alloy for Highly Active and Durable Bifunctional Electrocatalyst for Water Splitting under an Acidic Environment. Advanced Materials, 2023, 35(26) : 2300091.
[13] Chen Q, Han X, Xu Z, et al. Atomic phosphorus induces tunable lattice strain in high entropy alloys and boosts alkaline water splitting. Nano Energy, 2023, 110 : 108380.
[14] Fan L, Ji Y, Wang G, et al. High Entropy Alloy Electrocatalytic Electrode toward Alkaline Glycerol Valorization Coupling with Acidic Hydrogen Production. Journal of the American Chemical Society, 2022, 144(16) : 7224–7235.
[15] Huang K, Zhang B, Wu J, et al. Exploring the impact of atomic lattice deformation on oxygen evolution reactions based on a sub-5 nm pure face-centred cubic high-entropy alloy electrocatalyst . Journal of Materials Chemistry A, 2020, 8(24) : 11938–11947.